Lasers in Manufacturing Conference 2015

Characterization of the effect of laser scribing on the isolation coating of electrical steel

Peter Rauscher[a], Jan Hauptmann[a], Jörg Kaspar[a], Andreas Wetzig[a], Eckhard Beyer[a,b]

[a]*Fraunhofer IWS Dresden, Winterbergstrasse 28, 01277 Dresden, Germany*
[b]*TU Dresden, George-Bähr-Str. 3c, D-01069 Dresden, Germany*

Abstract

The demand for high energy efficiency leads to an ongoing development of better material grades of grain oriented electrical steel, which is used as core material in power or distribution transformers. In order to reduce the core losses of the silicon steel after the process of rolling different methods can be used, such as mechanical scratching, plasma irradiation, spark ablation and laser scribing. All these techniques induce mechanical or thermal stress that refines the magnetic domains. Due to the no-contact nature and the ease of integration laser scribing is the most commonly used technology, but with the drawback of laser-induced damage of the isolation layer [1], [2].
In this study the material ablation of the isolation layer due to high power continuous wave CO_2 (10.6 µm) and fiber laser beam sources (1.07 µm) was investigated in order to evaluate the damage threshold of the coating with respect to the treatment parameters. The study was performed with the so-called LMDR (Laser Magnetic Domain Refinement) test system to realize industry-related process parameters with spot velocities up to 300 m/s and laser output powers up to 4000 W. The experimental results are combined with material studies to characterize the ablation process related to the difference in the absorption behavior of the material based on the difference in wavelength [3].

Keywords: laser scribing; surface treatment; ablation; silicon steel

1. Introduction

Laser scribing of grain oriented electrical steel is used to improve the magnetic properties of silicon steel sheets that are used as core material in distribution or power transformers. The theoretical approach is the refinement of the magnetic domains by applying thermal induced local strains after the process of rolling. The primary objective of the so-called domain refinement methods is the reduction of the core loss. In addition, the isolation layer on the sheet surfaces should not be damaged or removed through the process in order to guarantee the insulating properties and corrosion resistance.

The surface defects due to laser scribing were investigated using continuous wave (cw) CO_2 laser beam sources and q-switched Nd:YAG laser beam sources [2, 4-6]. However, the development of high power, highly brilliant cw laser beam in the near infrared, like the fiber laser, enables new opportunities for the laser scribing process in terms of core loss improvement as well as the effect on the isolation layer, see [3, 7]. This study focuses on the surface defects produced by high power cw CO_2 and fiber laser and is based on the research results of [7]. The specific aim of this work was the evaluation of the threshold damage of the coating with respect to the treatment parameters and the used laser beam sources. Additionally, metallurgical examinations were carried out to observe the produced defects in order to characterize the process of the material removal.

2. Experimental procedure

2.1. Experimental setup

The experiments were performed on high permeability grain oriented electrical steel (comparable to M103-27P) using the so-called LMDR (Laser Magnetic Domain Refinement) test system developed and installed at the Fraunhofer IWS Dresden for continuous material treatment. The specification of the LMDR test system is summarized in Table 1. [8]

Table 1. Specification of the LMDR test system [8]

notation	specification
working width	up to 1000 mm
axis velocity	0.5 - 90 m·min^{-1}
laser spot velocity	up to 300 m·s^{-1}
laser beam sources	two laser beam sources selectable (CO_2 or fiber coupled solid state laser beam sources)
maximum laser power	1000 – 5000 W (dependent on the laser beam source)
line distance	2 – 20 mm
material	single sheets up to 1000 mm x 1000 mm

The focal spot of the LMDR test system is elliptically shaped. The semi-major axis R_Y is aligned along the scanning direction perpendicular to the direction of rolling. The semi-minor axis R_X is aligned along the direction of rolling and determines the width of the laser line on the sheet surface. The dimension of the spot depends on the optical configuration as well as on the used laser beam source. In order to evaluate the ablation of the coating independently of the optical configuration, the treatment parameters can be summarized to the mean intensity, defined as

$$\bar{I} = \frac{P_L}{\pi \cdot R_X \cdot R_Y} \qquad (1)$$

with P_L as laser power, R_X as the semi-minor axis of the elliptical spot and R_Y as the semi-major axis of the elliptical spot. In addition, the dwell time t_W is defined as follows

$$t_W = \frac{2 \cdot R_Y}{v_{Spot}} \qquad (2)$$

with v_{Spot} as spot velocity, R_Y as semi-major axis of the elliptical spot.

2.2. Experimental process

The experiments were performed with different laser beam sources as summarized in Table 2. The specific aim was the evaluation of the damage threshold of the coating in relation to the treatment parameters. Therefore, specific dwell time was selected by changing the spot velocity or the semi-major axis, as can be seen in equation (2).

Table 2. Specification of the used laser beam sources

	CO_2 laser	fiber laser (configuration 1)	fiber laser (configuration 2)	fiber laser (configuration 3)
maximum laser output power	3500 W	1800 W	4000 W	4000 W
fiber diameter		20 µm	50 µm	200 µm
BBP	3.5 mm x mrad	0.4 mm x mrad	1.5 mm x mrad	5 mm x mrad
wavelength	10.6 µm	1.07 µm	1.07 µm	1.07 µm

Subsequently, the output power of the laser beam sources was increased until the isolation layer was completely removed. The damage of the coating was evaluated optically for each treatment parameter based on the visibility of the laser lines. For the observation a digital light microscope was used. As a result, different damage classes were introduced to characterize the material ablation of the isolation layer similar to [7]. The defined damage classes are summarized in Table 3.

Table 3. Classification of visibility of the laser lines (damage categories) [7]

Class	notation	remarks
1	invisible laser lines	invisible laser lines on the sheet surface
2	visible laser lines	laser lines visible on the sheet surface with invisible basic material (Fe-Si matrix)
3	basic material visible	laser lines and basic material (Fe-Si matrix) visible

In order to evaluate the ablation process more precisely characteristic treated samples were selected for the scanning electron microscopy (SEM).

3. Results and Discussion

3.1. Threshold damage

For the investigated parameter range all 3 damage classes were observed in the case of the CO_2 laser, whereas the fiber laser produces almost the damage class 1 (invisible laser lines) and class 3 (basic material visible). For the evaluation of the material ablation, the threshold damage of the coating is defined as transition from damage class 1 (invisible laser lines) to damage class 3 (basic material visible) in case of the fiber laser and from damage class 2 (visible laser lines) to damage class 3 (basic material visible) in case of the CO_2 laser. The observed threshold damage indicates the complete removal of the coating for the investigated laser beam sources that is illustrated in Fig. 1.

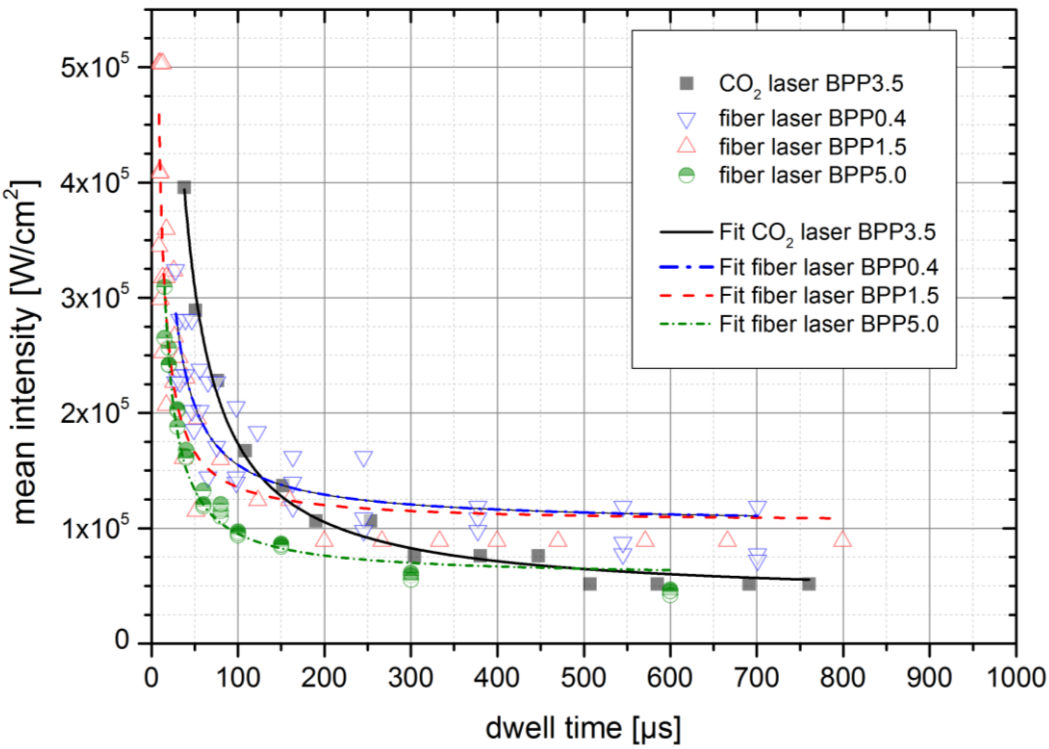

Fig. 1. Damage threshold of the coating as function of the mean intensity and dwell time for different laser beam sources (CO2 laser, fiber laser configuration 1 (BPP 0.4 mm x mrad), fiber laser configuration 2 (BPP 1.5 mm x mrad), fiber laser configuration 3 (BPP 5.0 mm x mrad))

The threshold damage depends on the used mean intensity as well as on the dwell time, as can be seen in Figure 1. The transition from damage class 1 (invisible laser lines) or damage class 2 (visible laser lines) to damage class 3 (basic material visible) was observed for all investigated laser beam sources. Additionally, a hyperbolic fit function was used to illustrate the dependence on the treatment parameters. If the dwell time exceeds a specific value, the threshold damage is almost independent on the mean intensity. Hence, an increase of the mean intensity destroys the isolation layer if the laser power is increased or the spot size is reduced, as can be seen equation (1). In contrast, short dwell times lead to a significant change of the threshold damage. Higher mean intensities can be used without affecting the isolation layer, which means that a higher laser power or smaller spot sizes can be used for an almost damage-free laser treatment.

Furthermore, the observed threshold damage of the coating shows no significant change between the fiber and the CO_2 laser due to the fact that the different absorption behavior is not considered. The calculation of the mean intensity, as shown in equation 1, does not take the absorption behavior of the silicon steel sheet into account. Hence, the output energy is considered and not the absorbed energy, which determines the material ablation. It is known from literature [4, 6] as well as from spectroscopic measurements [3] that the coating is almost transparent for the wavelength in the near infrared, like the fiber laser, and almost opaque in case of the CO_2 laser. This has to be taken into account, if the energy for the material ablation is of interest. From the application point of view, the parameter range for an almost damage-free laser treatment can be selected using the dependence summarized in Fig. 1.

3.2. Metallurgical analysis

The evaluation of the surface defects of the isolation layer was done on specific samples treated with fiber and CO_2 laser. As cross-section prepared samples were used for the scanning electron microscopy (SEM). The specific aim was the observation of the laser-affected zone due to the absorbed laser energy in order to characterize the process of the material ablation in greater detail. Therefore, typical samples that characterize the threshold damage have been selected, as can be seen in Table 3.

Table 4. Selected samples for the REM analysis

No	notation	damage class	Mean intensity In W/cm²	Dwell time in µs
1	FL_1	3 (basic material visible)	4.72E+05	41.5
2	FL_2	1 (invisible laser lines)	8.84E+04	27.7
3	CO_2_1	3 (basic material visible)	4.26E+05	38
4	CO_2_2	2 (visible laser lines)	1.22E+05	38

Fig. 2 and Fig. 3 show the laser line in cross-section for samples treated with the fiber laser, Fig. 4 and Fig. 5 show the laser line in case of the CO_2 laser. The laser-affected region is for all images almost in the center of the picture. The isolation layer on the top of the Fe-Si substrate consists of the forsterite layer and the phosphate layer as final layer on top, which has been analyzed with energy-dispersive X-ray spectroscopy (EDS). In order to locate the laser-affected zone in case of the fiber laser sample “FL2” (damage class 1, invisible laser lines), additional marks have been added before laser scribing process. Subsequently, the position was approximated to observe the samples in cross-section.

Dependent on the used laser beam source different observations were made. In case of the fiber laser the isolation layer is almost removed if the laser line becomes visible, as can be seen in Fig. 2. Dependent on the treatment parameters small remains of the isolation layer can be observed in the laser-affected zone. Additionally, the edge from the Fe-Si substrate to the coating is really sharp on both sides of the laser trace, similar to the observation in [7] for the altitude profile. In case of invisible laser lines, no laser trace was observed on the isolation layer as can be seen in Fig. 3. The sample shows no influence of the laser beam in the cross-section view.

The samples treated with the CO_2 laser show another behavior depending on the treatment parameters. The transition from the laser-affected zone to the Fe-Si substrate is more regular compared to the fiber laser. Furthermore, a small layer of the coating remains in the cross-section view and covers almost the whole laser trace, even if the sample was classified as class 3 (basic material visible), as it can be seen in Fig. 4. However, the coating in the laser-affected zone is molten, especially in the middle position of the laser trace, which can be related to the intensity distribution of the laser beam. In case of the sample, which has been classified with damage class 2 (visible laser lines), more of the isolation layer remains at the laser trace. Molten areas of the coating can be observed in the laser-affected zone, which are significantly smaller compared to Fig. 4.

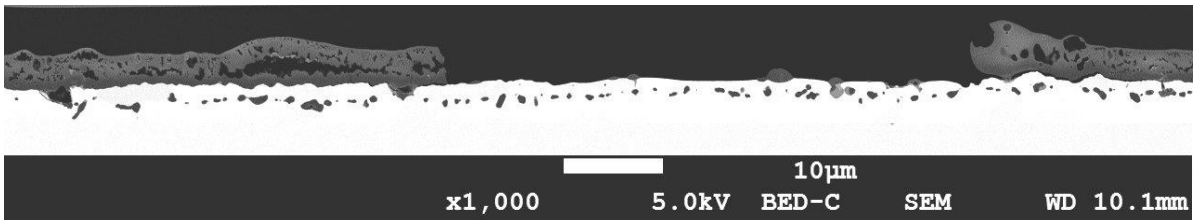

Fig. 2. SEM photograph of the laser line treated with the fiber laser beam source (configuration 2), damage class 3 (basic material visible); cross section; sample notation “FL_1”

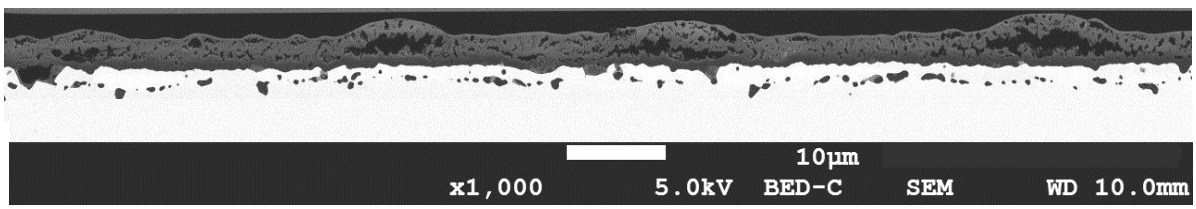

Fig. 3. SEM photograph of the laser line treated with the fiber laser beam source (configuration 2), damage class 1 (invisible laser lines); cross section; sample notation “FL_2”

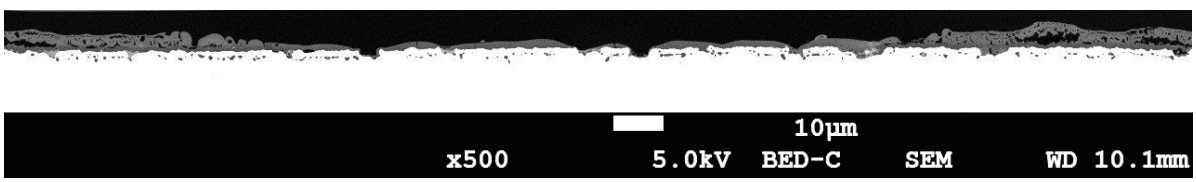

Fig. 4. SEM photograph of the laser line treated with the CO_2 laser beam source; damage class 3 (basic material visible), cross section; sample notation “CO_2_1”

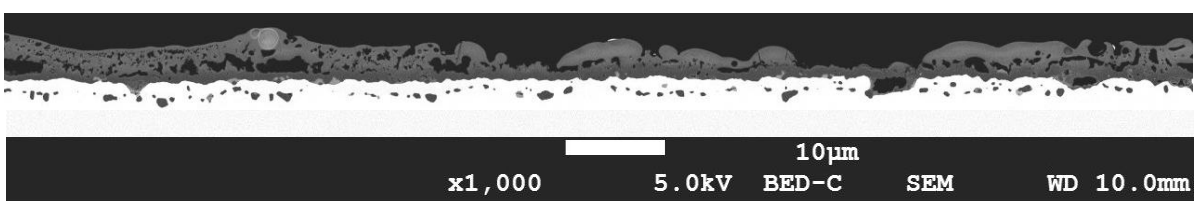

Fig. 5. SEM photograph of the laser line treated with the CO_2 laser beam source; damage class 2 (visible laser lines), cross section; sample notation “CO_2_2”

The SEM observations and the detected damage classes in combination with the spectroscopic measurement in [3] support the assumption that the material ablation is dependent on the used laser beam source related to the difference of the wavelength. The ablation process in case of the CO_2 laser is

continuous, starting from the top of the isolation layer. The remaining amount of the isolation layer depends on the used treatment parameters that mean that an increase of the used laser energy reduces the thickness of the isolation layer until the basis material becomes visible.

In opposite to the CO_2 laser, the energy of the fiber laser is almost transmitted through the coating and will be absorbed by the basic Fe-Si substrate. The isolation layer is almost removed, if the laser lines become visible. Hence, it can be assumed that ablation is more related to an abrupt explosive removal or chipping of the coating. The remains of the isolation layer, as can be seen in Fig. 2, can be attributed to re-deposited material after the laser process or even to unremoved parts of the isolation layer due to higher adhesion. The most obvious effect for the material ablation seems to be related to a gas expansion of vaporized coating due to an overheating on the interface of the Fe-Si substrate, which leads to chipping of the isolation layer.

4. Conclusion

The threshold damage of the coating was analyzed for different laser beam sources on grain oriented electrical steel in order to characterize a parameter range for an almost damage-free laser treatment. In this study the CO_2 and fiber laser beam sources were compared in terms of the material ablation. Both laser beam sources can produce invisible laser lines, but due to the difference in the absorption behavior of the coating different removal process were observed. The study has shown that the CO_2 laser leads to a gradual ablation, whereas the coating damage in case of the fiber laser results in an explosive removal or chipping of the isolation layer.

The knowledge of the threshold damage of the coating and the ablation process in dependence of the used laser beam source can be used for further improvements of the laser scribing process in terms of an almost damage-free treatment. The core loss improvement as objective aim of this additional treatment process has to be adapted to the specific process conditions in order to achieve both, high core loss improvement and damage-free laser treatment.

Acknowledgements

The investigation was performed in interdisciplinary cooperation with the Fraunhofer IWS Dresden, Rofin Sinar Laser GmbH and Maschinenfabrik Karl H. Arnold GmbH & Co. KG. We thank all involved persons for assistance and for comments that greatly improved the manuscript.

References

[1] Zhaosuo Xia, Yonglin Kang, Quanli Wang, Developments in the production of grain-oriented electrical steel (Journal of Magnetism and Magnetic Materials 320, 2008), pp. 3229-3233

[2] Weiderfeller, B.; Riehemann, W.; Mordike, B.I., Characterization of surface defects produced in transformer sheet by Nd:YAG radiation to reduce electrical losses (Lasers in Engineering, Vol.3,1994), pp. 87-98

[3] Rauscher, Peter; Hauptmann, Jan; Wetzig, Andreas; Beyer, Eckhard, Domain refinement of grain oriented electrical steel with high power laser beam sources (International journal of modern physics B, Vol.28 (2014), No.12, Art. 1442003, 11 pp.)

[4] G. Bán, G. Songini, G. Abburuzzese, New Methods for improving magnetic characteristics of grain-oriented electrical steel by laser scribing (Soft Magnetic Material, 16th conference, 2003, Düsseldorf)

[5] W. Tian, Y. Zhu, Z. Yuan,Z. Luo, Effect of laser scribing on grain-oriented silicon steel (2nd International Conference on Electronic & Mechanical Engineering and Information Technology (EMEIT-2012))

[6] G. C. Rauch, R. F. Krause, Effect of beam dwell time on surface changes during laser scribing, J. Appl. Phys. 57 (1).15 April 1985

[7] Rauscher, Peter; Schröder, Nikolai; Hauptmann, Jan; Wetzig, Andreas; Beyer, Eckhard: Effects of laser irradiation on the isolation layer of grain oriented electrical steel (International Conference on Magnetism and Metallurgy (WMM) <6, 2014, Cardiff>) In:

Schneider, J.: 6th International Conference on Magnetism and Metallurgy, WMM 2014: Cardiff, UK, June 17th to 19th, 2014. Cardiff: Spectrum Printing, 2014, pp. 434-441

[8] Rauscher, Peter; Hauptmann, Jan; Beyer, Eckhard; Laser scribing of grain oriented electrical steel under the aspect of industrial utilization using high power laser beam sources (Lasers in Manufacturing (LiM 2013), 2013, Munich) In: Physics Procedia, Volume 41, 2013, Pages 312–318